The American Journal of Pathology, Vol. 169, No. 5, November 2006

DOI: 10.2353/ajpath.2006.060006

Tumorigenesis and Neoplastic Progression

Individual Cell-Based Models of Tumor-Environment Interactions

Multiple Effects of CD97 on Tumor Invasion

Joerg Galle,* Doreen Sittig,† Isabelle Hanisch,† Manja Wobus,† Elke Wandel,†‡ Markus Loeffler,*§ and Gabriela Aust†

From the Interdisciplinary Center for Bioinformatics, the Institute for Medical Informatics, Statistics, and Epidemiology,§ the Center of Surgery,† Research Laboratories, and the Interdisciplinary Center of Clinical Research,‡ University of Leipzig, Leipzig, Germany*

The presence of scattered tumor cells at the invading front of several carcinomas has clinical significance. These cells differ in their protein expression from cells in central tumor regions as recently shown for the EGF-TM7 receptor CD97. To understand the impact of such heterogeneity on tumor invasion, we investigated tumor cells with modified CD97 expression *in vitro* and *in vivo*. Applying an individual cell-based computer model approach, we linked specific cell properties of these cells to tumor invasion characteristics. CD97 overexpression promoted tumor growth in *scid* mice, stimulated single cell motility, increased proteolytic activity of matrix metalloproteinases, and secretion of chemokines *in vitro* in an isoform-specific manner. We demonstrated by computer simulation studies that these effects of CD97 can increase the invasion capacity of tumors. Furthermore, they can cause the appearance of scattered tumor cells at the invasion front. We identified local tumor environment interactions as triggers of these multiple capabilities. Experimentally, our simulation results are supported by the finding that CD97 expression in tumor cells is regulated by their environment. Our combined experimental-theoretical analysis provides novel insight to how variations of individual cell properties can be linked to individual patterns of tumor cell invasion. ***(Am J Pathol 2006, 169:1802–1811; DOI: 10.2353/ajpath.2006.060006)***

The progression of carcinomas is associated with a loss of epithelial differentiation and gain of mesenchyme-like capabilities of scattered tumor cells at the invasive front. This transition is associated with alterations of the expression of molecules involved in cell-cell and/or cell-extracellular matrix interactions, such as motility-promoting molecules.[1–3] Furthermore, the secretion of cytokines and extracellular matrix-degrading proteinases are altered.[4,5] For colorectal carcinomas it has been shown that in metastases such alterations are reversed and the molecules show a similar expression pattern or level compared with the central region of the primary tumor.[6,7] Consequently, Brabletz and co-workers[6,7] suggested an active role of the tumor environment in malignant tumor progression. A tumor microenvironment invasion model was suggested by Condeelis and co-workers.[8]

It is a challenge to understand how the complex tumor invasion behavior emerges from collective interactions on the molecular and cellular level. Although the effects of molecular changes on the individual cell behavior can be quantified directly in experiments, dynamic links between the changes at the cellular level and the characteristics of the tumor invasion process are hard to assess. Here, we exclusively focus on that problem. A major insight into the link between individual cell behavior and tissue dynamics can be gained by computer modeling approaches. They permit investigation of the potential role of generic organization principles in specific tissues. We chose

Supported by the Deutsche Forschungsgemeinschaft (DFG; project AU 132/3-1 and grant BIZ-6 1/1 to J.G.) and by the Interdisciplinary Center of Clinical Research at the Faculty of Medicine of the University Leipzig (project D6).

Accepted for publication July 27, 2006.

E.W. is a fellow of the Interdisciplinary Center of Clinical Research Leipzig.

Supplementary material for this article can be found on *http://ajp.amjpathol.org*.

Address reprint requests to Joerg Galle, IZBI, Haertelstr. 16-18, 4107 Leipzig Germany. E-mail: galle@izbi.uni-leipzig.de.

individual cell-based models (IBMs[9,10]) to approach the challenge.

Considering the growth of tumor cell populations, a number of IBMs of the growth of tumor spheroids have been established.[11,12] Tumor invasion into stroma has been approached by cellular automatons[13] and lattice variants of IBMs.[14] Here, we introduce a novel class of lattice-free IBMs of the growth and collective invasion of carcinoma into stroma after breakdown of the basal membrane. On one hand, the approach enables us to analyze the impact of different cellular alterations on growth and invasion dynamics. On the other hand, we can study several assumptions about the origin of these alterations. We apply this approach to understand observations related to CD97 expression.

CD97 is a member of the EGF-7TM subfamily of class B G-protein-coupled receptors.[15,16] It consists of a variable number of N-terminally located EGF domains, a long extracellular stalk, the 7-transmembrane (7TM) domain, and a short intracellular C-terminal region. Alternative splicing results in three isoforms containing three (EGF 1,2,5), four (EGF 1,2,3,5), or five EGF domains (EGF 1-5). Several lines of evidence suggest a role of CD97 in tumor migration and invasiveness. CD97 shows stronger expression at scattered tumor cells of the invasion front of nearly half of colorectal carcinomas than in solid formations of the same tumor.[17] Normal colorectal epithelium is CD97-negative or only slightly positive. Furthermore, CD97 expression levels correlate with the *in vitro* migration and invasion capacity (chemotaxis) of colorectal tumor cell lines and model tumor clones.[17] In thyroid carcinomas, CD97 is related to dedifferentiation and tumor stage.[18]

Motivated by these results and further directed by the presented studies on isoform-specific tumor growth *in vivo*, we used CD97-transfected cells to investigate the effect of CD97 (EGF 1,2,5), C-terminal-truncated CD97 (EGF 1,2,5/TM1) and CD97 (EGF 1-5) (Figure 1A) on *in vitro* random cell motility, proteolytic activity, and chemokine secretion. We relate the results in the framework of our IBM, directly demonstrating the relevance of the observed effects in tumor invasion and the impact of the tumor environment in the process. We discuss our results with an emphasis on colorectal carcinomas.

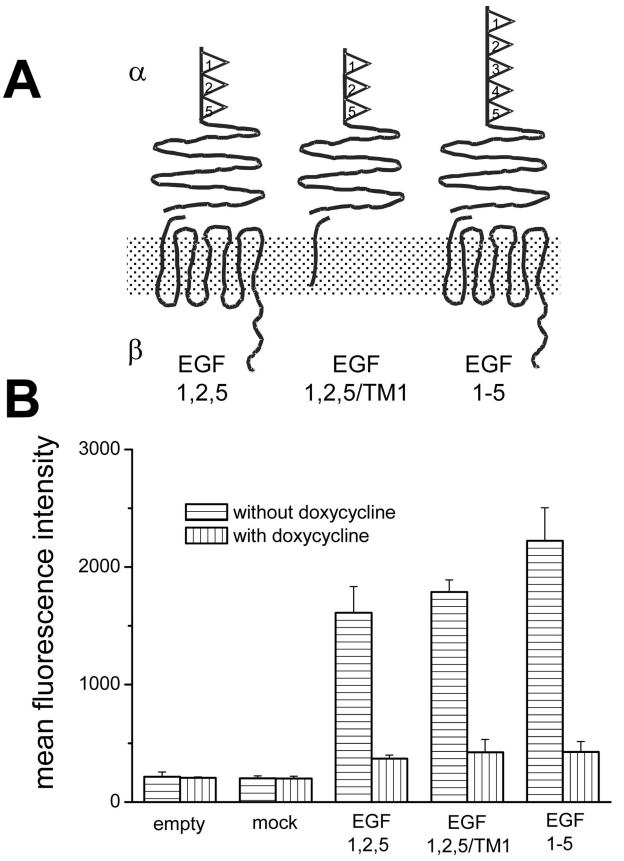

Figure 1. CD97 clones. **A:** Schematic structure of stably expressed CD97 molecules in HT1080 cells. CD97 consists of an α and β chain that are noncovalently bound. The CD97 (EGF 1,2,5) and CD97 (EGF 1-5) isoforms differ in their number of extracellular EGF domains. CD97 (EGF 1,2,5/TM1) is truncated within the first transmembrane domain. **B:** *In vitro* CD97 expression levels of the HT1080 clones cultured with and without doxycycline determined by flow cytometry (mean ± SEM, $n = 3$).

Materials and Methods

CD97-Expressing Cells

Tet-off HT1080 clones stably expressing CD97 (EGF 1,2,5), CD97 (EGF 1-5), or C-terminal-truncated CD97 (EGF 1,2,5/TM1) were generated as described.[17] Control cells contain only the empty plasmid or CD97 (EGF 1,2,5) mock. To induce the expression of the respective molecules, cells were cultured without doxycycline (Figure 1B). All clones additionally express enhanced green fluorescence protein (EGFP). Clones derived from wild-type Widr colorectal carcinoma cells were generated by stable transfection with the empty pEGFP-N1 vector (BD Biosciences, Heidelberg, Germany) or the plasmid encoding CD97 (EGF 1,2,5). Two clones for each transfected cDNA and cell type were selected out of 10 to 40 examining CD97 and EGFP expression by flow cytometry. Results of one clone are shown. Those of the other one were identical. The human tumor cell lines HT1080, Widr, DLD-1, Caco-2, and SW480 were obtained from the American Type Culture Collection (Rockville, MD).

Cell Cultures

For two-dimensional tumor colony monitoring, 1×10^3 cells were seeded in a six-well plate. For three-dimensional tumor colony monitoring, 1×10^3 cells were seeded into 0.25% agar/medium/20% fetal calf serum in a 24-well plate. Formed colonies were analyzed every 24 hours throughout at least 14 days using digital light microscopy. In two-dimensional colonies cell doubling times were observed by analyzing the initial exponential growth phase. In selected colonies, proliferation was determined after 14 days using the BrdU Labeling and Detection Kit II (Roche Diagnostics GmbH, Mannheim, Germany). The effect of cell density on CD97 expression in two-dimensional cultures was determined by fluores-

Table 1. *Scid* Mice Groups

Group	HT1080 cells, stably transfected	Number of animals	Doxycycline treatment
1	Empty plasmid	8	−
2	Empty plasmid	8	+
3	CD97 (EGF 1,2,5)	8	−
4	CD97 (EGF 1,2,5)	8	+
5	CD97 (EGF 1,2,5/TM1)	8	−
6	CD97 (EGF 1,2,5/TM1)	8	+
7	CD97 (EGF 1-5)	8	−
8	CD97 (EGF 1-5)	8	+

All animals underwent a subcutaneous injection with different tet-off HT1080 stably transfected clones. Every second animal group received doxycycline every third day to maintain down-regulation of CD97.

cence-activated cell sorting analysis in nonconfluent single cell and 90% confluent cultures after 48 hours.

Characterization of the Single Cell Motility

Cells (5×10^2 cells/cm^2) were seeded in 96-well plates. In nine independent series, the position of 30 cells was detected at several times (t) using digital light microscopy starting 4 hours after plating. Within the time between the measurements (dt), a migrating cell changes its position and thus changes its distance to all cells of the selected group. We calculated the change of the distances $\Delta d_{ij} = d_{ij}(t) - d_{ij}(t + dt)$ between all pairs i,j of cells in a group. For cells undergoing an independent Brownian random walk, it turns out that $<(\Delta d_{ij})^2>$, the average of $(\Delta d_{ij})^2$, grows linearly with time. We confirmed that time dependence and derived a migration coefficient D by calculating $D = <(\Delta d_{ij})^2>/8dt$ for $dt = 12$ hours.

Interleukin (IL)-8 Enzyme-Linked Immunosorbent Assay and Sodium Dodecyl Sulfate-Substrate Gel Electrophoresis (Zymography)

Supernatants of 1×10^5 cells cultured in 500 μl of OPTI-MEM (Invitrogen, Karlsruhe, Germany) without and with tumor necrosis factor (TNF)-α (5 ng/ml; ImmunoTools, Friesoythe, Germany) were assayed for IL-8 (ELISA; Bender MedSystems, Vienna, Austria). Gelatin zymography of the supernatants was performed as described.[19] Specific MMP activity was checked by adding 10 mmol/L ethylenediaminetetraacetic acid to the developing buffer.

Scid Mice

HT1080 tumor cells (1.5×10^6) in 150 μl of phosphate-buffered saline were injected subcutaneously between the scapulae of the BALB/c severe combined immunodeficient scid/scid (*scid*) mice, 5 to 6 weeks old. Each HT1080 clone was injected into two groups of eight animals (Table 1). To maintain down-regulation of CD97 in one of these groups, doxycycline (0.01 mg/g body weight) was injected subcutaneously every third day. The mice were controlled every second day for tumor growth and state of health and were sacrificed when the tumor had reached maximal growth (~10% of the actual body weight of the animal or more then 2 cm^3), started to ulcerate, or 100 days after tumor cell injection. Tumors were cryopreserved in liquid nitrogen. Expression of CD97 in the tumors was verified by immunohistology.

Immunohistology and Flow Cytometry

The CD97 monoclonal antibody (mAb) CLB-CD97/3 detects an epitope within the stalk region (CD97^{stalk}).[15] For immunohistology, serial sections were cut to 6 μm and fixed in ice-cold methanol for 10 minutes. The sections were incubated with the primary antibody (Ab) (4°C, overnight). Bound Abs were detected with a supersensitive detection system (Vector Laboratories, Burlingame, CA). Microvessel density was analyzed by anti-CD31 (Santa Cruz Biotechnology, Heidelberg, Germany) staining as described.[20]

In flow cytometry, cells were phenotyped with the desired Ab by indirect immunofluorescence using F(ab′)$_2$ goat anti-mouse immunoglobulin-phycoerythrin or streptavidin-phycoerythrin (DAKO, Hamburg, Germany) in the case of a biotinylated Ab. The antigen levels were determined as mean fluorescence intensity of stained cells in comparison to cells stained with an isotype-matched but irrelevant mAb.

Results

CD97 Clones

Tet-off HT1080 cells stably containing the empty plasmid or CD97 (EGF 1,2,5) mock showed basal CD97 expression in flow cytometry (Figure 1). The established clones CD97 (EGF 1,2,5), CD97 (EGF 1-5), or C-terminal truncated CD97 (EGF 1,2,5/TM1) showed a 6- to 10-fold overexpression of the respective CD97 forms compared with CD97 (EGF 1,2,5) mock clones. CD97 overexpression in CD97 (EGF 1,2,5), CD97 (EGF 1-5), or C-terminal truncated CD97 (EGF 1,2,5/TM1) clones was significantly reduced by doxycycline (Figure 1B).

CD97 (EGF 1,2,5) Alters Tumor Growth in Scid Mice

The induced tumors were found to grow confined within the subcutis. CD97 expression in tumors was confirmed by immunohistology. CD97 (EGF 1,2,5), (EGF 1-5), and (EGF 1,2,5/TM1) tumors were CD97^{stalk}-positive. Tumors of mice treated with doxycycline and all tumors derived from empty cells were CD97^{stalk}-negative or only slightly positive because of the basal CD97 expression in wild-type tet-off HT1080 cells (not shown).

Assuming a linear growth of the radius R of tumor spheroids,[12] we analyzed the macroscopic tumor growth quantitatively, calculating the extrapolated start time (t_0) and the growth velocity (v) (Figure 2A). We found that CD97 (EGF 1,2,5) overexpression propagated tumor growth compared with controls, whereas CD97 (EGF,

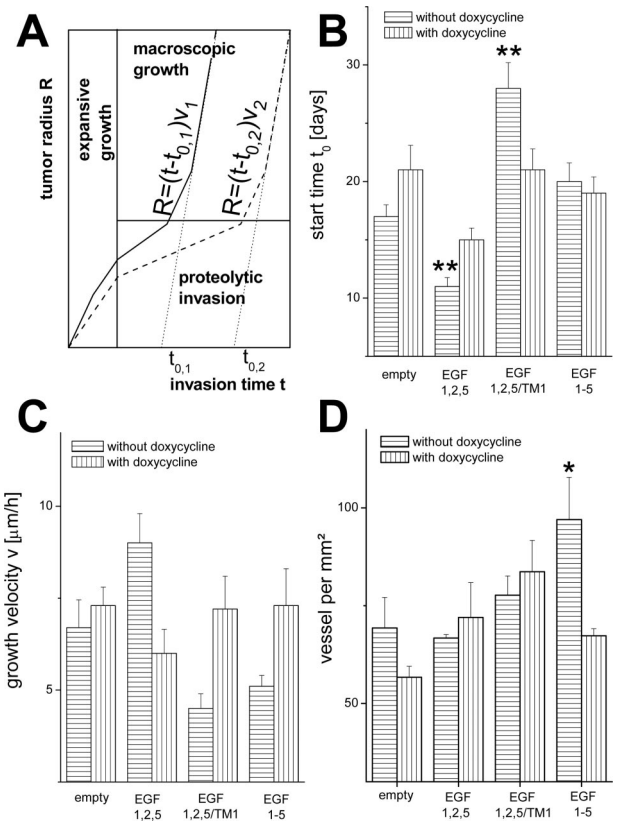

Figure 2. *In vivo* tumor growth. **A:** Sketch of a simplified model of tumor propagation in *scid* mice. An initial expansive growth phase is followed by a phase of proteolytic invasion. After releasing strong tissue confinements, a phase of rapid macroscopic growth starts. The phases are shown for two tumors (tumors 1 and 2), in which tumor 1 (solid line) is more invasive. **B** and **C:** Estimated tumor growth parameters. **B:** Starting time t_0; **C:** growth velocity v derived from a linear fit to the tumor radius $R = (t - t_0)v$ in the phase of macroscopic growth ($n = 8$, mean ± SEM). **D:** Microvessel density determined by CD31 staining in histological sections of various HT1080 tumors ($n = 8$, mean ± SEM). Significance of a change compared with the empty control system: $^*P < 0.05$, $^{**}P < 0.01$; Westfall-Young test.[42]

1,2,5/TM1) reduces it (Figure 2, B and C). Decrease of CD97 expression by doxycycline reduces the observed effects depending on the CD97 iso- or truncated forms. Because tumor vascularization can promote growth and invasion, we analyzed vascularization by CD31 staining. We found an increased microvessel density in tumors induced with HT1080 CD97 (EGF 1-5) cells, whereas the density was equal between CD97 (EGF 1,2,5), CD97 (EGF 1,2,5/TM1), and the control cells (Figure 2D). Thus, the observed tumor growth was not determined by vascularization.

Multiple Effects of CD97 on Tumor Cell Properties

Although we found no significant differences in the doubling times of HT1080 clones *in vitro* [empty: 23 ± 3 hours; CD97 (EGF 1,2,5) mock: 24 ± 4 hours; CD97 (EGF 1,2,5): 23 ± 3 hours; CD97 (EGF 1,2,5/TM1): 21 ± 3 hours; CD97 (EGF 1-5): 23 ± 4 hours; mean ± SD, $n = 7$, cultivation without doxycycline], we observed molecule-specific changes of cell properties regarding single cell motility, proteolytic activity, and chemokine secretion. The effects presented in the following were confirmed by measurements of cells precultured with doxycycline to decrease CD97. The decrease of the respective molecules by doxycycline reduced the effects gained by their overexpression. Furthermore, all effects induced by CD97 (EGF 1,2,5) were confirmed in Widr clones (not shown).

CD97 (EGF 1,2,5) Promotes Single Cell Motility

In vitro single cells of all clones investigated showed a Brownian-like random migration. We found an increase of the cell migration coefficient (D) by a factor of ~3 to 4 in CD97 (EGF 1,2,5) HT1080 cells compared with empty control or CD97 (EGF 1,2,5) mock cells (Figure 3A). In contrast, CD97 (EGF 1-5) cells showed a nearly unaffected and CD97 (EGF 1,2,5/TM1) cells even a reduced motility.

CD97 (EGF 1,2,5) Stimulates Proteolytic Activity

Considering that MMPs are hardly regulated at post-transcriptional level by cytokines, tissue inhibitors of MMPs (TIMPs) and cleaving to generate the active forms, we estimated proteolytic activity by zymography. In unstimulated cultures, the highest activity was found in CD97 (EGF 1,2,5) cells (Figure 3B). After stimulation with TNF-α, CD97 (EGF 1,2,5) cells especially secreted elevated levels of pro-MMP9 (92 kd) and its active 82-kd form. In addition, the active glycosylated 62-kd and unglycosylated 59-kd forms of pro-MMP2 (72 kd) could be found. No bands were visible after adding ethylenediaminetetraacetic acid to the gels (not shown).

CD97 (EGF 1,2,5) Increases Chemokine Secretion

IL-8 expression by colorectal carcinoma cells was shown to increase during tumor progression[5] and to improve cell growth.[21] We measured IL-8 secretion *in vitro*. CD97 (EGF 1,2,5) cells showed the highest basal secretion and time-dependent increase of IL-8 (Figure 3C). Because CD97 (EGF 1,2,5) and CD97 (EGF 1-5) cells differ in their extracellular domain only, IL-8 secretion may be triggered by this part of the molecule. This assumption is supported by cells expressing truncated CD97 (EGF 1,2,5/TM1), which also showed high IL-8 levels. TNF-α stimulated IL-8 secretion in all HT1080 clones. The highest effect was again found in CD97 (EGF 1,2,5) cells (not shown).

Modeling the Growth of Tumor Cell Colonies

We investigated the impact of the multiple cellular alterations induced by CD97 (EGF 1,2,5) on tumor invasion by applying a computational approach based on the IBM of growth regulation of epithelial cell populations recently introduced by us.[9] In this model the cells are represented by elastic objects. They are able to move, to grow, and to

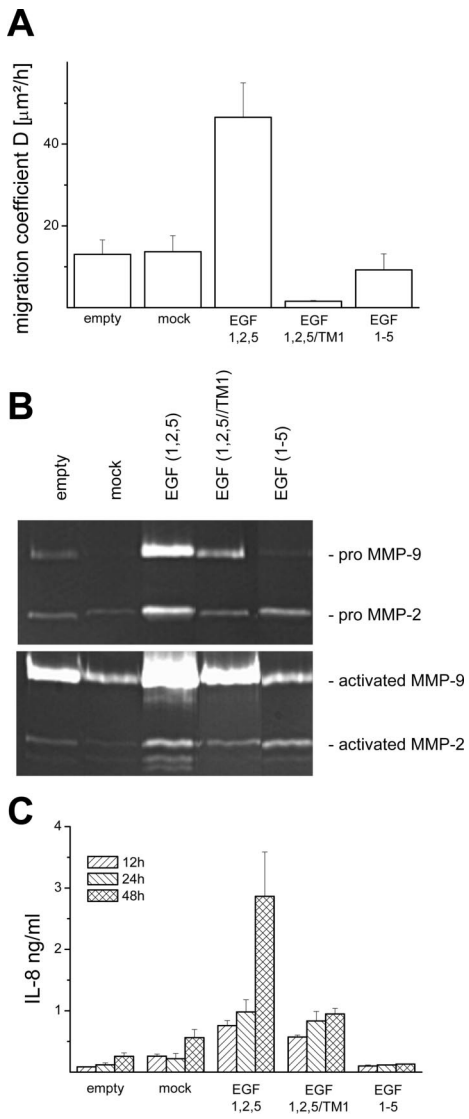

Figure 3. *In vitro* properties of the HT-1080 clones. **A–C:** Single cell properties of HT1080 clones cultured without doxycycline. CD97 (EGF 1,2,5) stimulates single cell motility and increases proteolytic activity of matrix metalloproteinases and chemokine secretion. **A:** Single cell migration coefficients calculated for a time span of 12 hours (n = 9, mean ± SEM). **B:** Gelatin zymograms of supernatants of unstimulated (top row) and TNF-α-stimulated (bottom row) HT1080 clones. **C:** Time-dependent basal IL-8 secretion (n = 3, mean ± SEM).

divide and can form adhesive contacts with neighbor cells and matrix components. The loss of cell-matrix contacts induces programmed cell death and impedes proliferation. Cell compression results in quiescence via contact inhibition of growth. Details can be found in the online supplemental material (see *http://ajp.amjpathol.org*).

Parameterization

The computer model cells are characterized by a set of experimentally accessible biomechanical and cell-biological parameters. We derived the majority of these parameters from literature.[9] The remaining ones were determined in growth experiments of tumor cell clones, forcing the model to reproduce the colony growth dynamics of Widr control cells. Two phases can be distinguished during colony growth *in vitro*[9]: an initial phase in which the number of cells grows exponentially, allowing derivation of the cell doubling times, and a subsequent phase in which the colony diameter grows linearly, ie, with a constant spreading velocity. In the computer model we used the cell doubling times as intrinsic cell growth time τ. Experimentally, we found two morphologically identical subpopulations (SP), SP_{fast} and SP_{slow}, of Widr control cells. Their doubling times were the same (21 ± 3 hours, mean ± SD, n = 7), but SP_{fast} spread faster than SP_{slow}. We assumed that the subpopulations are characterized by different capabilities to escape contact inhibition of growth.[22] In our computer model cells undergo contact inhibition of growth if their volume is compressed by their neighbor cells below the threshold volume V_{inh} (Figure 4A). We assumed a smaller value of V_{inh} for the subpopulation SP_{fast} compared with SP_{slow} (see supplemental material, Table S1, at *http://ajp.amjpathol.org*), ie, we assumed that SP_{fast} is less sensitive to contact inhibition of growth. This results in a quantitative description of the colony growth even regarding the distribution of proliferation events (Figure 4, B and C).

Regulation I: Contact Inhibition of Migration

We have shown that CD97 (EGF 1,2,5) transfectants are characterized by an increased single cell random migration coefficient D. However, in a growing population spatially restricted activation of cytoskeleton reorganization could cause a directed migration.[23] Thus, we considered two cases in our model: a fully random migration of the cells and a locally directed migration at the colony boundary, where each migration step is assumed to point out of the colony. In computer simulations, we found that an increased random migration had negligible effects on the spreading of a colony, whereas a stimulated directed migration significantly promoted that process (not shown).

Analyzing the colony growth behavior of the CD97 (EGF 1,2,5) clones *in vitro* without stroma, we found no promoting effect on spreading. The spreading of the CD97 (EGF 1,2,5) clones could be described by that of clones of control cells, considering the slightly different doubling time of the transfected cells (25 ± 3 hours, mean ± SD, n = 7) only (Figure 4, D and E). The result implies that the cells either perform an enhanced random migration or are subjected to contact inhibition of migration. This is supported by the formation of smooth colony boundaries as found for controls (compare Figure 4B).

Regulation II: Contact Inhibition of Growth

A model of tumor invasion requires a representation of the tumor stroma. For that purpose, we introduced so-called stroma cells, which represent both cell and matrix components of the stroma. We expand a population of these cells until it fills a closed box inducing a persistent within-tissue pressure. This pressure keeps the stroma cells quiescent because of contact inhibition of growth.

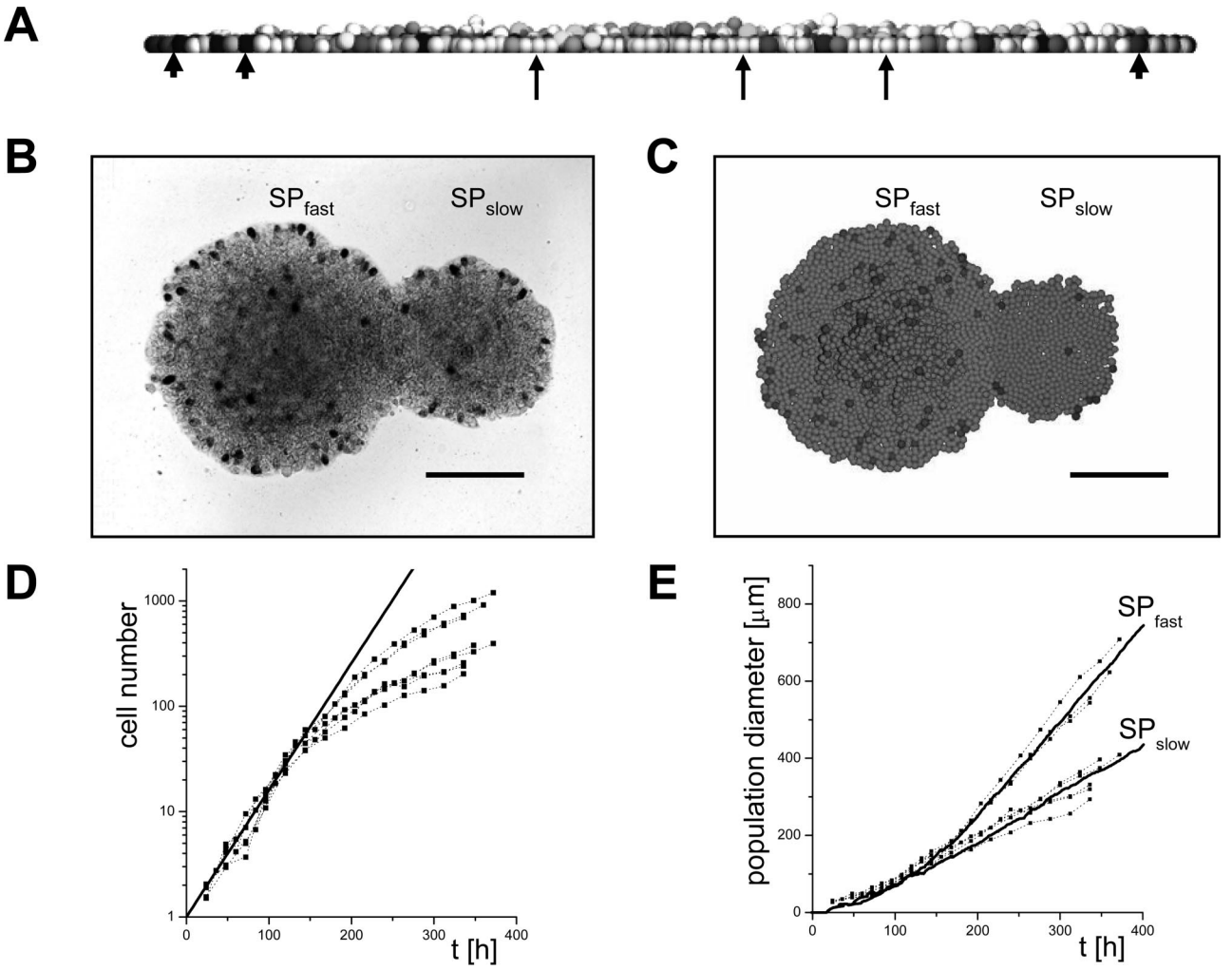

Figure 4. Experimental and computer-simulated colony growth. **A:** Vertical section through a growing computer model population. The gray value of the cells is a marker of the cell volume. Black cells (**arrowheads**) are in the act of starting division; white cells (**arrows**) underwent contact inhibition of growth; ie, they are quiescent because of compression by neighboring cells. **B:** Top view on two cultured Widr empty control populations after 14 days stained for proliferation by BrdU. They grow from cells of different subpopulations (SP_{fast}, SP_{slow}). **C:** Computer simulation results related to **B**. **D:** Cell number of CD97 (EGF 1,2,5)-transfected Widr cell colonies versus time *t*. The thick line indicates exponential growth according to a cell doubling time of 25 hours. **E:** Diameter of the colonies shown in **D**. Lines are computer simulation results applying the parameter sets of Widr empty control cells for SP_{fast} and SP_{slow} and considering the doubling time of the transfected cells. Scale bars = 200 μm.

An initial tumor is generated selecting a few cells at the center of the box and changing their parameters. We used the parameter sets of Widr empty control cells as reference sets. For the tumor cells we used the set of subpopulation SP_{fast} and for the stroma cell that of SP_{slow}, assuming for tumor cells a decreased sensitivity to contact inhibition of growth.[24] This growth advantage enables them to expand under the initial conditions. All other parameters are identical, facilitating further comparative analysis.

Tumor spheroids in a stable polymer matrix stop growing at a certain diameter that corresponds to a threshold pressure acting on the population and inducing a defined compression.[25] In *in vitro* experiments, we found that tumor spheroids of both CD97-transfected and control Widr cells stopped growth at a diameter of ~200 ± 20 μm (mean ± SD, n = 30, not shown). This indicates that in these cells contact inhibition of growth is identically regulated.

Modeling Collective Tumor Cell Invasion

Subsequent to tumor growth we investigated the impact of tumor cell motility, proteolytic activity, growth, and survival on collective tumor invasion. For specific tumor-stroma interaction parameters (see below), we assumed reasonable values ensuring that the invasion velocity is significantly smaller than the growth velocity of an unconfined tumor cell colony.

Loss of Contact Inhibition and Proteolytic Activity of Tumor Cells Are Prerequisites of Invasion

In our computer model reference tumors stop growth if their expansion results in a pressure in the system high enough to induce contact inhibition of growth in the tumor cells (Figure 5, A–C). To escape that kind of growth inhibition, tumor cells have to degrade their surrounding stroma. Thus, we assumed that stroma cells can be degraded by

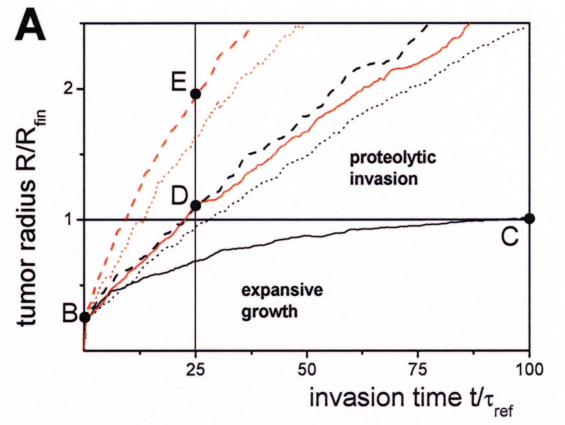

assumed characteristics of the simulated system							
active tumor cell proteolysis		-	x	x	x	x	x
doubled tumor cell growth time		-	-	x	-	-	-
increased tumor cell migration activity	random	-	-	-	x	-	-
	directed	-	-	-	-	x	x
tumor cell apoptosis		-	-	-	-		x

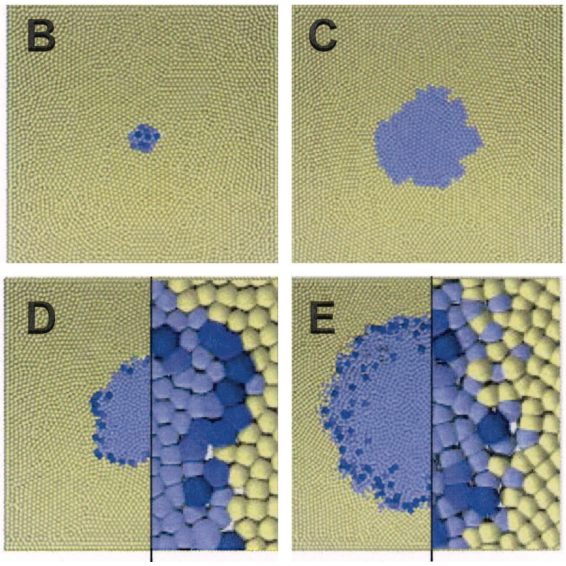

Figure 5. Computer model results on tumor invasion. **A:** Effects of tumor cell properties on invasion dynamics. The tumor radius R is scaled with the finite tumor radius R_{fin} obtained without stroma degradation (black solid line); the time t with the reference cell growth time τ_{ref} of 21 hours. **B–E:** Snapshots of computer-simulated tumors at the selected times points indicated in **A**. Tumor cells are blue; stroma cells are yellow. Color saturation indicates immanent cell division. Without proteolytic activity of the tumor cells (**A**, black solid line) tumor expansion starting from a small initial tumor (**B**) stops because of contact inhibition of growth after ~100 τ_{ref} (**C**). Proteolytic activity of the tumor cells (**A**, black dashed line) enables persistent tumor invasion. Thus, the tumor radius reaches the value of R_{fin} already after ~25 τ_{ref} (**D**). The invasion is only moderately slowed, doubling the tumor cell growth time τ (**A**, black dotted line). In contrast to enhanced random migration (**A**, red solid line), enhanced directed migration in the presence of active proteolysis (**A**, red dashed line) strongly promotes invasion by roughening the proteolytic active interface (compare magnifications in **D** and **E**). Regardless of that large interface, stroma contact-induced tumor cell apoptosis has only weak effects on invasion (**A**, red dotted line). Box height: 800 μm (**B–E**); magnifications; 160 μm (**D**, **E**).

adjacent, proteolytically active tumor cells with a defined rate w_{prot} per cell-cell contact. Changes of the proteolytic activity of tumor cells are modeled changing this rate w_{prot}.

In simulations we found that considering proteolysis the initial growth phase is followed by an invasion phase (Figure 5, A and D). During proteolytic invasion we found an approximately linear increase of the tumor radius R with time that is proportional to the degradation rate w_{prot}. The process requires the assumed partial loss of contact inhibition in tumor cells. Without that growth advantage, proteolytic tumor invasion is inhibited by stroma self-regeneration (not shown).

Tumor Cell Growth Rates and Survival Have Minor Relevance for Invasion

As a complementary process to stroma degradation, the tumor environment may affect tumor cell growth and survival. Thus, we studied effects of changed tumor cell growth time τ and assumed that stroma cell contacts may induce tumor cell apoptosis with a rate w_{apop} per cell-cell contact. An increase of the growth time τ of all tumor cells decreases the tumor invasion speed. However, because the invasion on large time scales is determined by the local stroma degradation, changes of τ have only moderate effects on the invasion dynamics (Figure 5A). The slower the tumor cells cycle, the more of them escape contact inhibition and start growing and expanding into the available space. In an analogous way, apoptosis of tumor cells at the invasion front with rate w_{apop} is compensated by stimulated tumor cell proliferation and consequently has only moderate effects on the invasion dynamics (Figure 5A).

Increased Tumor Cell Motility Can Promote Collective Invasion

Although CD97 (EGF 1,2,5) overexpression in Widr does not induce a directed migration at the population boundary *in vitro*, we studied the impact of both elevated random and directed cell migration on tumor invasion assuming that the cell polarization required for directed migration is caused by specific tumor-stroma interactions. In computer simulations, we found that elevated random migration has negligible effects on invasion (Figure 5A). Assuming an orientation of the migration at the tumor invasion front causes a front morphology characterized by scattered cells and protruding cell clusters (Figure 5E). Thus, in case of proteolytically active tumor cells, directed migration increases the degradation capacity of the tumor by increasing the tumor-stroma interface and consequently strongly promotes invasion (Figure 5, A and E).

On the Origin of CD97 Expression in Vivo

The studies presented above demonstrate that all CD97 (EGF 1,2,5)-induced effects can promote invasion. It remains an open question, whether the observed CD97

staining in colorectal carcinomas results from single cell mutations or an environmental regulation process.

Clones of Highly Motile Cells Expand Rapidly

To mimic a mutation of selected tumor cells independent of their environment, we assumed that these cells are characterized by a modified parameter set. Focusing on cell migration we assumed for mutated cells a four times increased migration coefficient and directed migration induced by tumor-stroma interactions. Remarkably, the clone of a single mutated cell at the tumor front can spread within a short time throughout the front (Figure 6A). Computer simulations showed that although mutated cells that bud into the stroma rarely proliferate, these cells immediately start efficiently cycling if they become encapsulated by other tumor cells. We found that the clones of mutated cells spread faster than those of unaltered cells. Thus, they determine the entire tumor with time. Such a conversion was not found for tumor cells strongly stained for CD97. Consequently, we introduced an alternative approach.

Environmentally Regulated Tumor Cell Motility

We assumed that all tumor cells are regulated by their local environment. We modeled such regulation assuming the parameter set of each tumor cell to reversibly depend on the number of its tumor cell neighbors. We introduce a threshold number of tumor cell neighbors below which the parameter set of the tumor cell changes; ie, we assume a density-dependent regulation. We again focused on altered migration. In a series of simulations, we observed that altered migration (four times increased migration coefficient, directed migration) as mutated migration significantly strengthens invasion. Interestingly, we again found that altered cells at the tumor front rarely proliferate. The assumed environmental regulation generates an invasion front where only front cells exhibit altered cell properties (Figure 6, B–D). For a threshold number of approximately four to six in a layer, this distribution approaches that observed in colorectal carcinomas for cells strongly stained for CD97 (Figure 6E). This suggests a related mechanism *in vivo*.

CD97 (EGF 1,2,5) in Tumor Cell Lines Is Density Regulated

To confirm our hypothesis, we examined CD97 expression in wild-type colorectal carcinoma cell lines during their growth to confluence by flow cytometry. We found that in all cell types CD97 expression was significantly reduced in cells forming a confluent layer compared with nonconfluent, single cell cultures (Figure 6F). This result was independent of the absolute expression levels of CD97. This indicates that CD97 is regulated in a density-dependent manner, at least *in vitro*.

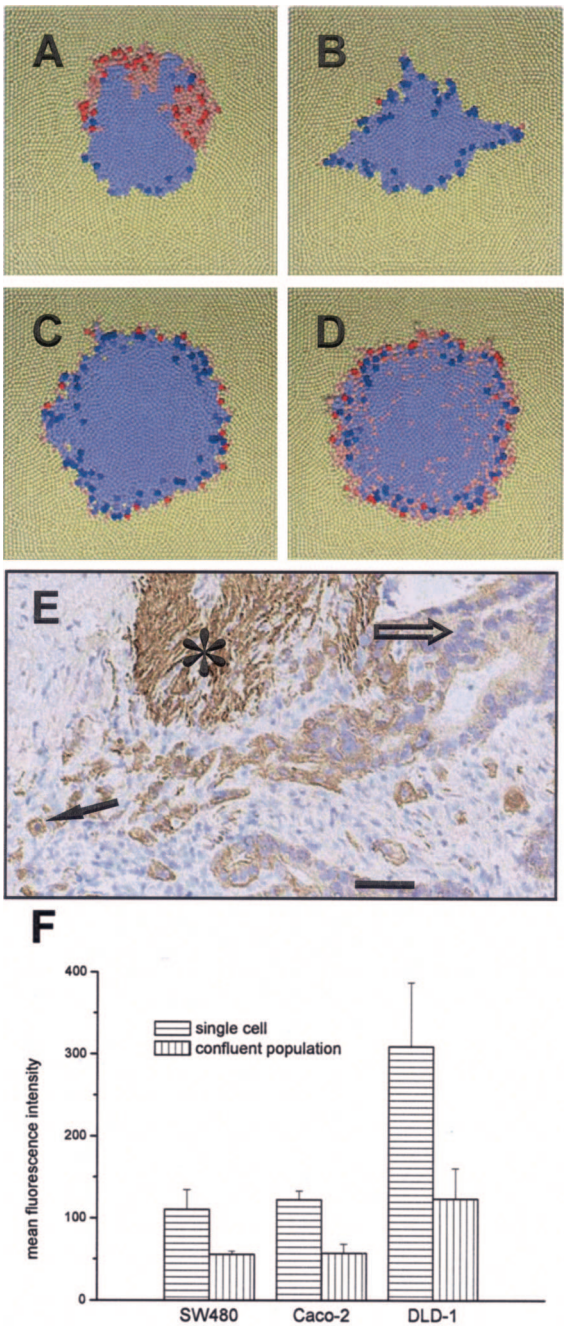

Figure 6. On the origin of increased CD97 expression in scattered tumor cells at the invasion front of colorectal carcinoma. Top view on computer model systems after an invasion time of 25 reference cell growth times of 21 hours. Altered cells (red) are characterized by a four times increased migration coefficient and a directed migration at the tumor invasion front. Saturated color indicates imminent cell division. **A:** Invasion after a mutation (stable alteration) of a single cell. The clone of that cell has spread partially throughout the tumor front. **B–D:** Invasion considering regulated alteration. Tumor cells become altered if the number of tumor cell neighbors falls below two (**B**), four (**C**), and six (**D**), respectively. Accordingly, altered cells occur at the tumor front. This corresponds to the expression of CD97 found in colorectal carcinoma (**E**). Stronger expression of CD97 is found in scattered tumor cells or tumor cell groups (**arrow**) surrounded by stroma compared with tumor cells located in tumor glands or solid tumor trabecula (**open arrow**). Smooth muscle cells (**asterisk**) also express CD97.[43] **F:** CD97 expression in colorectal carcinoma cell lines, here shown for SW480, Caco-2, and DLD-1 cells, forming confluent layers is significantly decreased compared with that in single cell cultures of the same cell type as shown by flow cytometry (mean ± SEM, $n = 3$). The result does not depend on absolute CD97 expression levels. Box height, 800 μm (**A–D**). Scale bar = 50 μm.

Discussion

We demonstrated a migration- and tumor growth-promoting effect of CD97. However, this effect was seen only for CD97 (EGF 1,2,5), not for CD97 (EGF 1-5) or the C-terminally truncated CD97 (EGF 1,2,5). The specificity of the regulation suggests that the extracellular as well as the transmembrane domains and/or C-terminal region of the protein are involved. Regarding the *scid* mice experiments, our results exclude vascularization as a promoting factor of tumor growth, which we found most pronounced for CD97 (EGF 1-5), in agreement with Wang and co-workers.[26] The observed stimulation of random cell motility by CD97 (EGF 1,2,5) may explain why the molecule promotes cell migration and invasion in Boyden chamber assays as found by us.[17] We expect comparable results for any common chemoattractant of the considered colorectal tumor cells.

In several studies tumor budding, ie, the occurrence of scattered tumor cells at the tumor invasion front or host interface, was discussed as prognostic marker for reduced overall survival.[27,28] Here, we demonstrate that budding in carcinoma is a consequence of locally directed migration of highly motile tumor cells. Notably, the weak proliferation found in scattered tumor cells in colorectal carcinoma[7,29] and skin cancer[30] is reproduced by our model without additional assumptions. In the model, it arises as a consequence of the high motility of these cells modifying the cell-environment interaction and thus affecting cell compression. Our simulations demonstrate that the budding process does not require stable, long-range chemogradients. However, CD97-related budding requires stroma signaling to induce a directed migration at the tumor front. In colorectal carcinoma, the CD97 ligand CD55[31,32] or non-CD97-specific ligands as accumulating collagen I[6] may act as trigger. Note that this not implies a strong adhesive tumor-stroma interaction as often assumed to be required for invasion.[13] In the case that long-range chemogradients arise in the stroma, the highly motile scattered cells may very efficiently follow them and spread to distant places.[33] Thus, these cells in principle indicate a high risk of metastasis and postoperative recurrence. According to the density-dependent regulation, one would expect that metastases of colorectal carcinomas show the same staining of CD97 as the primary tumor as found for other molecules.[6,7]

The proteolytic activity of tumor cells was frequently used as a marker to predict tumor recurrence in several types of tumors.[34,35] Here, we demonstrated that in spatially homogeneous carcinoma increased proteolytic activity promotes tumor expansion. However, we expect that an imbalance in the quantitative expression of the proteases rather than an overall change of their expression may affect prognosis. In this case, tumor invasion could be hampered by nondegradable stroma components that accumulate at the tumor front. As a consequence the tumor cells would be forced to adapt their invasion mechanisms.[36]

Previous studies in several carcinomas have reported that an increased rate of proliferation is correlated with a less favorable prognosis.[37,38] However, low proliferation was also demonstrated to indicate reduced response to treatment, suggesting that tumors with elevated proliferation would have better response.[39] Moreover, according to recent studies,[40,41] in colorectal carcinoma a high Ki-67 value even constitutes a prognostic marker for low recurrence. We here provide an explanation for this apparent contradiction demonstrating that during proteolytic invasion the fraction of cycling cells depends on the balance between tumor cell proliferation, apoptosis, and stroma degradation. Thus, for fixed degradation rates a large fraction refers either to slow cycling times of the tumor cells or to their apoptosis. Consequently, in this specific case a high fraction of proliferating tumor cells signals a low capability to spread to distant places or a good response to treatment in agreement with results in colorectal carcinoma.[40,41] The finding of poor prognosis[37,38] may be related to an increased proteolytic activity of the tumor.

Applying our IBM, we derived a number of predictions about the impact of individual cell properties on tumor invasion dynamics. Assuming reasonable values for the tumor-stroma interaction parameters, these predictions regard the qualitative behavior. Quantitative models require a detailed specification of the heterogeneous stroma. This will be part of future model extensions. In summary, our experimental and theoretical results give a straight forward explanation why cells strongly stained for CD97 scatter at the invasion front of colorectal carcinoma and why the occurrence of these cells is related to poor prognosis. The higher expression of CD97 at the invasion front found in nearly half of colorectal carcinomas is suggested to be a result of an environmentally regulated, reversible expression of that molecule. More generally, our simulation results suggest that proteolytic activity at the tumor front in conjunction with elevated and directed cell motility are key steps to aggressive tumor invasion. High tumor cell proliferation rates in this context are not the cause but a consequence of invasion. Our findings may have major implications for the understanding of tumor invasion and prognostic factor analysis.

Acknowledgments

We thank J. Hamann (Academic Medical Center, University of Amsterdam, Amsterdam, The Netherlands) for providing the CD97 (1,2,5/TM1) plasmid and the CLB-CD97/3 mAb; and U. Schumacher and S. Feldhaus (Institute of Anatomy, University Hospital Eppendorf, Hamburg, Germany) for first screening experiments with *scid* mice.

References

1. Thiery JP: Epithelial-mesenchymal transitions in tumor progression. Nat Rev Cancer 2002, 2:442–454
2. Bates RC, Mercurio AM: The epithelial-mesenchymal transition (EMT) and colorectal cancer progression. Cancer Biol Ther 2005, 4:365–370
3. LaGamba D, Nawshad A, Hay ED: Microarray analysis of gene expression during epithelial-mesenchymal transformation. Dev Dyn 2005, 234:132–142

4. Balkwill F: Cancer and the chemokine network. Nat Rev Cancer 2004, 4:540–550
5. Bates RC, DeLeo III MJ, Mercurio AM: The epithelial-mesenchymal transition of colon carcinoma involves expression of IL-8 and CXCR-1-mediated chemotaxis. Exp Cell Res 2004, 299:315–324
6. Brabletz T, Spaderna S, Kolb J, Hlubek F, Faller G, Bruns CJ, Jung A, Nentwich J, Duluc I, Domon-Dell C, Kirchner T, Freund JN: Down-regulation of the homeodomain factor Cdx2 in colorectal cancer by collagen type I: an active role for the tumor environment in malignant tumor progression. Cancer Res 2004, 64:6973–6977
7. Brabletz T, Jung A, Reu S, Porzner M, Hlubek F, Kunz-Schughart LA, Knuechel R, Kirchner T: Variable beta-catenin expression in colorectal cancers indicates tumor progression driven by the tumor environment. Proc Natl Acad Sci USA 2001, 98:10356–10361
8. Wang W, Goswami S, Sahai E, Wyckoff JB, Segall JE, Condeelis JS: Tumor cells caught in the act of invading: their strategy for enhanced cell motility. Trends Cell Biol 2005, 15:138–145
9. Galle J, Loeffler M, Drasdo D: Modelling the effect of deregulated proliferation and apoptosis on the growth dynamics of epithelial cell populations in vitro. Biophys J 2005, 88:62–75
10. Galle J, Aust G, Schaller G, Beyer T, Drasdo D: Individual cell-based models of the spatio-temporal organisation of multicellular systems—achievements and limitations. Cytometry A 2006, 69:704–710
11. Schaller G. Meyer-Hermann M: Multicellular tumor spheroid in an off-lattice Voronoi/Delaunay cell model. Phys Rev E 2005, 71:051910
12. Drasdo D, Höhme S: Individual-based approaches to birth and death in avascular tumors. Math Comput Model 2003, 37:1163–1175
13. Alacron T, Byrne HM, PK Maini: A cellular automaton model for tumour growth in inhomogeneous environment. J Theor Biol 2003, 225:257–274
14. Turner S, Sherratt JA: Intercellular adhesion and cancer invasion: a discrete simulation using the extended Potts model. J Theor Biol 2002, 216:85–100
15. Kwakkenbos MJ, Kop EN, Stacey M, Matmati M, Gordon S, Lin HH, Hamann J: The EGF-TM7 family: a postgenomic view. Immunogenetics 2004, 55:655–666
16. Bjarnadottir TK, Fredriksson R, Hoglund PJ, Gloriam DE, Lagerstrom MC, Schioth HB: The human and mouse repertoire of the adhesion family of G-protein-coupled receptors. Genomics 2004, 84:23–33
17. Steinert M, Wobus M, Boltze C, Schutz A, Wahlbuhl M, Hamann J, Aust G: Expression and regulation of CD97 in colorectal carcinoma cell lines and tumor tissues. Am J Pathol 2002, 161:1657–1667
18. Hofmann A, Laue S, Rost AK, Scherbaum WA, Aust G: mRNA levels of membrane-type 1 matrix metalloproteinase (MT1-MMP), MMP-2, and MMP-9 and of their inhibitors TIMP-2 and TIMP-3 in normal thyrocytes and thyroid carcinoma cell lines. Thyroid 1998, 8:203–214
19. Aust G, Hofmann A, Laue S, Rost A, Kohler T, Scherbaum WA: Human thyroid carcinoma cell lines and normal thyrocytes: expression and regulation of matrix metalloproteinase-1 and tissue matrix metalloproteinase inhibitor-1 messenger-RNA and protein. Thyroid 1997, 7:713–724
20. de Jong JS, van Diest PJ, Baak JP: Hot spot microvessel density and the mitotic activity index are strong additional prognostic indicators in invasive breast cancer. Histopathology 2000, 36:306–312
21. Xie K: Interleukin-8 and human cancer biology. Cytokine Growth Factor Rev 2001, 12:375–391
22. Rubin H: Selected cell and selective microenvironment in neoplastic development. Cancer Res 2001, 61:799–807
23. Etienne-Manneville S: Cdc42—the centre of polarity. J Cell Sci 2004, 117:1291–1300
24. Trosko JE, Ruch RJ: Cell-cell communication in carcinogenesis. Front Biosci 1998, 3:d208–d236
25. Helmlinger G, Netti PA, Lichtenbeld HC, Melder RJ, Jain RK: Solid stress inhibits the growth of multicellular tumor spheroids. Nat Biotechnol 1997, 15:778–783
26. Wang T, Ward Y, Tian L, Lake R, Guedez L, Stetler-Stevenson WG, Kelly K: CD97, an adhesion receptor on inflammatory cells, stimulates angiogenesis through binding integrin counterreceptors on endothelial cells. Blood 2005, 105:2836–2844
27. Park KJ, Choi HJ, Roh MS, Kwon HC, Kim C: Intensity of tumor budding and its prognostic implications in invasive colon carcinoma. Dis Colon Rectum 2005, 48:1597–1602
28. Nakanishi Y, Ochiai A, Kato H, Tachimori Y, Igaki H, Hirohashi S: Clinicopathological significance of tumor nest configuration in patients with esophageal squamous cell carcinoma. Cancer 2001, 91:1114–1120
29. Palmqvist R, Rutegard JN, Bozoky B, Landberg G, Stenling R: Human colorectal cancers with an intact p16/cyclin D1/pRb pathway have up-regulated p16 expression and decreased proliferation in small invasive tumor clusters. Am J Pathol 2000, 157:1947–1953
30. Svensson S, Nilsson K, Ringberg A, Landberg G: Invade or proliferate? Two contrasting events in malignant behavior governed by p16(INK4a) and an intact Rb pathway illustrated by a model system of basal cell carcinoma. Cancer Res 2003, 63:1737–1742
31. Li L, Spendlove I, Morgan J, Durrant LG: CD55 is over-expressed in the tumour environment. Br J Cancer 2001, 84:80–86
32. Hamann J, Vogel B, van Schijndel GM, van Lier RA: The seven-span transmembrane receptor CD97 has a cellular ligand (CD55, DAF). J Exp Med 1996, 184:1185–1189
33. Condeelis J, Segall JE: Intravital imaging of cell movement in tumors. Nat Rev Cancer 2003, 3:921–930
34. Sato H, Takino T, Miyamori H: Roles of membrane-type matrix metalloproteinase-1 in tumor invasion and metastasis. Cancer Sci 2005, 96:212–217
35. Vihinen P, Kahari VM: Matrix metalloproteinases in cancer: prognostic markers and therapeutic targets. Int J Cancer 2002, 99:157–166
36. Friedl P, Wolf K: Tumor-cell invasion and migration: diversity and escape mechanisms. Nat Rev Cancer 2003, 3:362–374
37. Trihia H, Murray S, Price K, Gelber RD, Golouh R, Goldhirsch A, Coates AS, Collins J, Castiglione-Gertsch M, Gusterson BA: International Breast Cancer Study Group. Ki-67 expression in breast carcinoma: its association with grading systems, clinical parameters, and other prognostic factors—a surrogate marker? Cancer 2003, 97:1321–1331
38. Fernandez-Figueras MT, Puig L, Musulen E, Gilaberte M, Ferrandiz C, Lerma E, Ariza A: Prognostic significance of p27Kip1, p45Skp2 and Ki67 expression profiles in Merkel cell carcinoma, extracutaneous small cell carcinoma, and cutaneous squamous cell carcinoma. Histopathology 2005, 46:614–621
39. Imdahl A, Jenkner J, Ihling C, Ruckauer K, Farthmann EH: Is MIB-1 proliferation index a predictor for response to neoadjuvant therapy in patients with esophageal cancer? Am J Surg 2000, 179:514–520
40. Allegra CJ, Paik S, Colangelo LH, Parr AL, Kirsch I, Kim G, Klein P, Johnston PG, Wolmark N, Wieand HS: Prognostic value of thymidylate synthase, Ki-67, and p53 in patients with Dukes' B and C colon cancer: a National Cancer Institute-National Surgical Adjuvant Breast and Bowel Project collaborative study. J Clin Oncol 2003, 21:241–250
41. Garrity MM, Burgart LJ, Mahoney MR, Windschitl HE, Salim M, Wiesenfeld M, Krook JE, Michalak JC, Goldberg RM, O'Connell MJ, Furth AF, Sargent DJ, Murphy LM, Hill E, Riehle DL, Meyers CH, Witzig TE: North Central Cancer Treatment Group: prognostic value of proliferation, apoptosis, defective DNA mismatch repair, and p53 overexpression in patients with resected Dukes' B2 or C colon cancer: a North Central Cancer Treatment Group Study. J Clin Oncol 2004, 22:1572–1582
42. Eszlinger M, Krohn K, Berger K, Lauter J, Kropf S, Beck M, Fuhrer D, Paschke R: Gene expression analysis reveals evidence for increased expression of cell cycle-associated genes and Gq-protein-protein kinase C signaling in cold thyroid nodules. J Clin Endocrinol Metab 2005, 90:1163–1170
43. Aust G, Wandel E, Blotze C, Sittig D, Schutz A, Horn L-C, Wobus M: Diversity of CD97 in smooth muscle cells. Cell Tissue Res 2006, 324:139–147